Heat Disipation Balancig in Switched Reluctance Drives by Combined Use of Active and Passive Thermal ControlMethods

Alecksey Anuchin
Department of Electric Drives
Moscow Power Engineering Institute
Moscow, Russia
anuchin.alecksey@gmail.com

Fernando Briz
Department of Electrical, Electronic, Computers and Systems Engineering
University of Oviedo
Gijón, Spain

Igor Gulyaev
Electronics and Nanoelectronics Department
Ogarev Mordova State University
Saransk, Russia

Alexandr Zharkov
Department of Electric Drives
Moscow Power Engineering Institute
Moscow, Russia

Maria Gulyaeva
Department of Electric Drives
Moscow Power Engineering Institute
Moscow, Russia

Viktoriya Popova
Electronics and Nanoelectronics Department
Ogarev Mordova State University
Saransk, Russia

***Abstract*—Air-cooled heatsinks for electric drives often suffer from unbalances in the heat dissipation capability when several power modules are mounted on the same heatsink, eventually limiting the output power to that dictated by the hottest module. This paper discusses the options for the placement of the power modules on the heatsink for the particular case of switched reluctance drives. Combined with active thermal control methods, this reduces the temperature dispersion, and therefore allowso toincrease the maximum output power of the converter.**

Keywords— active thermal control, pulse-width modulation, switching losses, voltage source inverters, switched reluctance drive

I. INTRODUCTION

Most industrial drives are based on a voltage source inverters, where IGBT power modules share a common heatsink. The design with separate modules for each inverter leg is normally utilized for powers of 30 kW and higher. Switched reluctance drive (SRD) having 3 phases needs six power modules: three top-side choppers and three bottom-side choppers. While losses in all power modules during operation of the drive are expected to be the same, the heat dissipation capability for the different modules can vary due to dispersion in heatsink parameters. For example, if the configuration shown in Fig. 1 is used, the air flowing along ribs becomes hotter when reaching the farthest power module. Therefore, the temperature of this farthest module is expected to be the highest.

The current control in the windings of switched reluctance motor (SRM) is usually performed using hysteresis current controllers. There are three modes of operation:

- both switches are on, and the full DC-link voltage is applied to the motor winding (see Fig. 2a);
- one switch is on and another is off, and the phase is short-circuited with zero voltage applied (see Fig. 2b and c);
- both switches are off, and the negative DC-link voltage is applied to the winding through freewheeling diodes, while current continue flowing in the winding (see Fig. 2d).

The research was performed with the support of the Russian Science Foundation grant (project 15-19-20057).

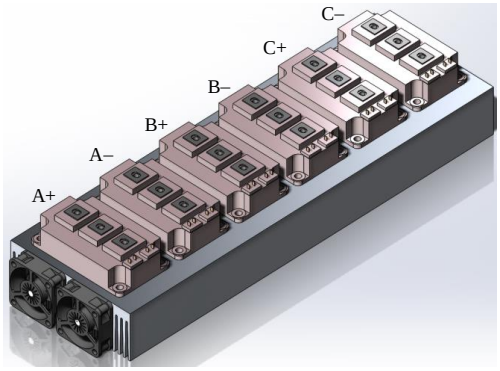

Fig. 1. Typical configuration of the power converter with forced air-cooling for SRM.

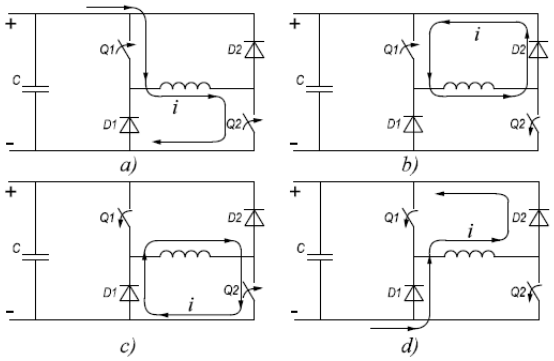

Fig. 2. Operation modes of a single phase of SRD.

Thermal conditions of the drive can be affected by means of active thermal control [2]–[5], which can be used to improve thermal conditions of the semiconducting devices. These methods are mostly focused on thermal stabilization rather than on the decrease in temperature of a particular component of the inverter. There are various PWM strategies that enable a decrease of switching losses in the system [6]–[8]. In [9] the model predictive control strategy was used to redistribute losses from the hottest power module to the coldest, but this method is limited by the conventional three-phase inverter applications with sinusoidal shape of the output current. For SRD the active thermal control methods were not considered due to less degrees of freedom compared to conventional inverters.

In [1] the analysis of the thermal configuration was performed in order to improve its thermal conditions. The reliability issues of SRD were considered in [10] and [11] where the electrothermal models were used for representation of the thermal model of power electronics converter.

This paper considers a two-stage optimization of the thermal behavior of SRDs. The first stage relays on the proper configuration of the power converter, which helps to equalize the average temperature of the power module of each phase. The second stage defines the control principles for hysteresis current controller aimed to remove unbalances between power modules, consequently contributing to increase the maximum output power of the converter. The proposed method is verified using simulation model of the SRD.

II. SRD Modeling

A. Electrical model of SRD

The most popular configuration of the three-phase SRD has 6/4 topology (see Fig. 3) with six teeth stator and four teeth rotor. Each stator tooth has its coil. Two opposite coils connected serially or in parallel form the stator phase winding. Each phase is fed from its own asymmetrical bridge inverter which forms an unipolar current in it. The typical operation cycle for a single phase starts in the position with the smallest inductance (curve *A* in Fig. 4a). The hysteresis current controller stabilizes current on a referenced value. During the rotor rotation the phase inductance changes till it reaches its maximum value (curve *B* in Fig. 4a). In this point the phase should be switched off. The mechanical work is equal to the area "*oabo*".

For the simplification of the equations of the model the relationship between the flux linkage and the current was linearized (see Fig. 4b) [12]. It was assumed that the phase inductance changes according to the following equation:

$$L = L_0 - \Delta L \cos\theta, \tag{1}$$

where L_0 is the average inductance, ΔL is the half difference between maximum and minimum inductances, and θ is the electric rotor angular position.

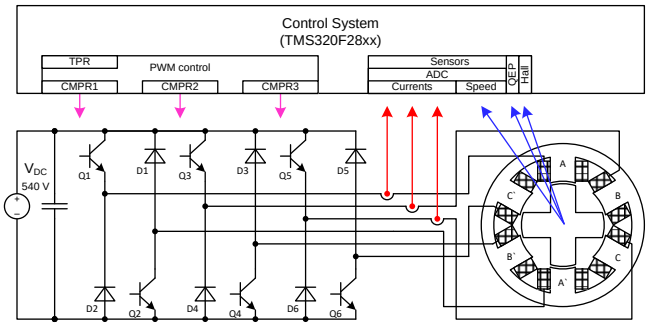

Fig. 3. SRD configuration.

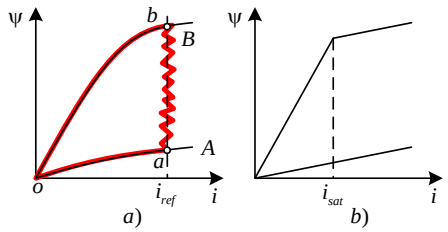

Fig. 4. Relationship between flux linkage and current (a—for a real motor; b—for the linearized motor model).

The switched reluctance machines are designed to work in saturation. This gives better efficiency and better power factor. The saturation current in the model is the same for any rotor position. If the phase current reaches the saturation current level the differential inductance becomes equal to the minimal phase inductance as it is shown in Fig. 4b. This is relatively rude approximation but for the purpose of this model it is acceptable.

The flux linkage of each phase, which are assumed to be magnetically independent, can be evaluated by the following equation:

$$\frac{\mathrm{d}\psi}{\mathrm{d}t} = v - iR, \tag{2}$$

where v is the voltage applied, i is the phase current, and R is the active resistance of the winding. This equation is implemented using Euler integration method:

$$\psi_k = \psi_{k-1} + (v - iR)h, \tag{3}$$

where ψ_k and ψ_{k-1} are the new and previous flux linkages respectively, and h is the integration step size.

The power converter from Fig. 3 can produce only positive current in any phase, and this should be checked in case of zero or negative voltage is applied (Fig. 2b, c, and d). Thus, it should be checked if the flux linkage value became negative:

$$\psi_k = \begin{cases} \psi_k, \psi_k \geq 0; \\ 0, \psi_k < 0. \end{cases} \tag{4}$$

The estimated flux linkage is used to evaluate the value of the current flowing in the phase winding:

$$i = \frac{\psi}{L}. \tag{5}$$

This current can be smaller or bigger than the value of the saturation current. If it is smaller, then the motor operates in linear region and no any correction is needed. If it is larger, the machine is in the saturation, and the actual value of the phase current should be corrected by:

$$i = I_{sat} + \frac{\psi - L \cdot I_{sat}}{L_{min}}, \tag{6}$$

where I_{sat} is the saturation current, and L_{min} is the minimum inductance of the winding. As there is no need to evaluate torque and mechanical parameters of the motor, the torque equation is not implemented.

B. Losses model in the power converter

Power losses in power converters can be split between conductive and switching.. Conduction losses for transistor (7) and diode (8) are obtained by multiplying the current by the voltage drop, which is obtained from a look-up table provided in the transistor data sheet [13]:

$$\Delta P_{Q\,cond} = i \cdot \mathrm{v_{CE}}(i, \tau), \tag{7}$$

$$\Delta P_{D\,cond} = i \cdot \mathrm{v_F}(i, \tau), \tag{8}$$

where $\mathrm{v_{CE}}$ is the collector to emitter voltage drop as a function of flowing current i and temperature τ; $\mathrm{v_F}$ is the diode forward characteristics.

Each commutation performed by control system results in switching losses occurring in transistor and/or reverse recovery losses in the freewheeling diode. According to [13] these losses are represented in joules, and converted into watts by:

$$\Delta P_{Q\,on} = E_{on}/h, \tag{9}$$

$$\Delta P_{Q\,off} = E_{off}/h, \tag{10}$$

$$\Delta P_{D\,rr} = E_{rr}/h, \tag{11}$$

where E_{on}, E_{off}, and E_{rr} are turn on, turn off and reverse recovery energies, and $\Delta P_{Q\,on}$, $\Delta P_{Q\,off}$, and $\Delta P_{D\,rr}$ are turn on, turn off, and reverse recovery loss powers.

C. Thermal model of the forced air-cooled heatsink

The thermal model (see Fig. 5) obtains losses ΔP_n from six power modules located at the top of the heatsink. The heatsink itself is split into six parts of some having some thermal capacitance C_n. Each of these six parts is connected with adjoining parts by some thermal resistance R_{m-m} (module to module) and heat is extracted through R_{m-a} (module to ambient). The cooling air temperature varies as it passes along the ribs of the heatsink. Assuming that the airflow is constant, the air increases its temperature at each part of the heatsink with respect to the difference between temperature of this part τ_n and the incoming air temperature $\tau_{air\ n}$ multiplied by k_τ, which depends on the airflow rate and thermal capacitance of the air.

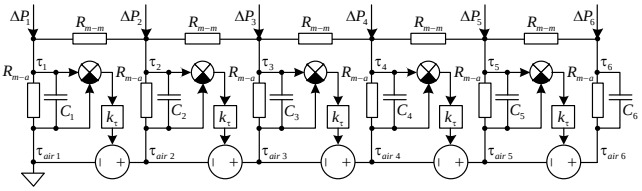

Fig. 5. Thermal model of the forced air-cooled heatsink.

III. Thermal Control of the Power Converter for SRD

A. Passive thermal control

The original configuration of the power modules shown in Fig. 1 suffers from overheat of the phase C. These power modules are located in the hottest part of the heatsink. And the maximum output power is limited by the temperature of the hottest power module. For the SRD it is not possible to redistribute the losses between different phases without having impact to the produced torque as it can be done in three-phase AC drives [9]. But still it is possible to relocate power modules in order to make active thermal control possible.

Fig. 6 shows the configuration of the power converter where the "A–" and "C–" phase connections are swapped. In this configuration phase A contains the coldest and hottest power modules. The average temperature of two modules of any phase will be equal to the average temperature of other phase modules. And between different modules of the phase redistribution of losses can be done using active thermal control.

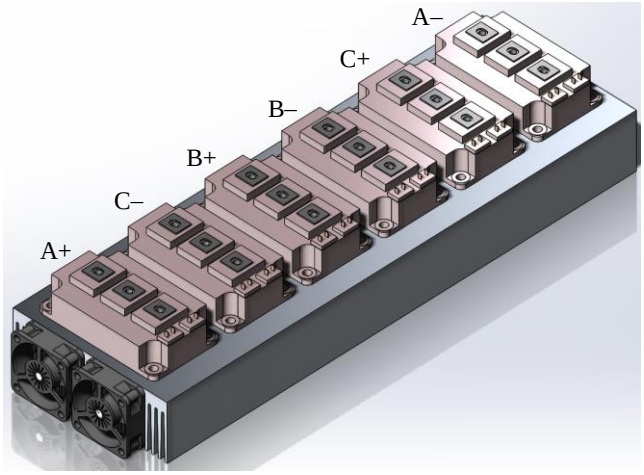

Fig. 6. Suggested configuration of the power converter for SRD.

B. Active thermal control

The current regulation in the phases of SRD in most cases is implemented using hysteresis controller. The motor produces positive torque when the phase inductance has positive derivative. Thus, the commutation cycle starts when the phase inductance is small by applying the voltage according to Fig. 2a. The current of the phase grows, and it should be stabilized when reaching the reference value by switching to a different state represented in Fig. 2b, c, or d. The state from Fig. 2d is commonly used only at the final stage of the commutation cycle, when it is needed to decrease current rapidly, and during operation in the regenerative mode.

Considering two options in Fig. 2b and c, when the phase of the motor is short-circuited, and the zero voltage is applied, the choice between them can be dictated by the thermal conditions of the particular power modules. For example, if the power module of phase "A–" with low-side chopper has higher temperature than the power module of phase "A+", then it is preferable to commutate high-side chopper Q1 in moving to state from Fig. 2c. This helps to move switching losses to the coldest module of this motor phase. The flowchart for the suggested control strategy is presented in Fig. 7.

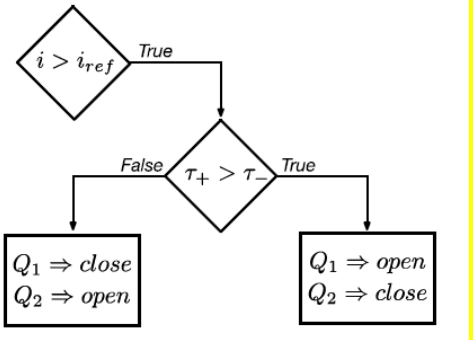

Fig. 7. Active thermal control strategy for a single phase of SRD.

IV. Simulation Results

The simulation model was implemented in C++ Builder, and it has the parameters as shown in Table I. Thermal capacitance of the heatsink is decreased by more than 1000 times to shorten the simulation time.

TABLE I. TABLE TYPE STYLES

Parameter	*Value*	*Units*
C_1, C_2, C_3, C_4, C_5, and C_6	0.1	$\frac{\text{J}}{\text{kg}\times\text{K}}$
R_{m-m}	0.5	K/W
R_{m-a}	0.75	K/W
k_τ	0.054	-
h	1/120000	s
L_{min}	0.001	H
L_{max}	0.01	H
I_{sat}	20	A
n	1000	rpm
pole pairs	4	-
R	0.05	Ohm
I_{ref}	60	A
V_{DC}	600	V

The operation of the drive in the original configuration from Fig. 1 is shown in Fig. 8. The temperature of the power modules grows with the distance from the air inlet. The temperature of the power modules is affected by the control strategy and the modules with low-side chopper have higher temperature due to extra switching losses.

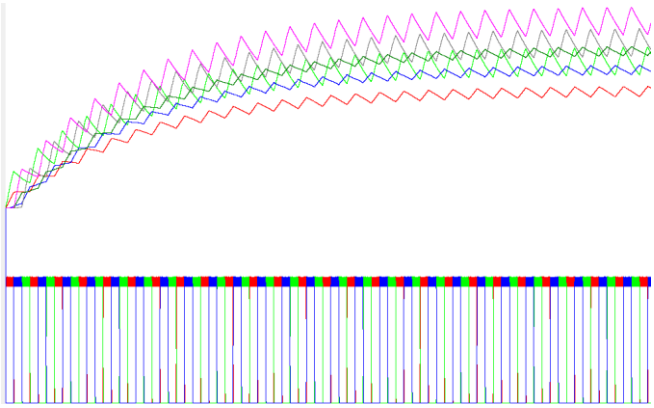

Fig. 8. Operation of the drive in the original configuration and current controller which commutates low-side chopper. Temperatures of the modules A+, A–, B+, B–, C+, and C– shown with red, lime, blue, gray, green, and fuchsia respectively. Currents of phases A, B, and C at the bottom graph.

Changing power converter configuration to the presented in Fig. 6 results in significant growth of the modules with low-side choppers (see Fig. 9). They were all moved to the hottest side of the heatsink and the hysteresis current controller is switching these modules to stabilize the phase current at the reference value increasing their temperature by adding switching losses.

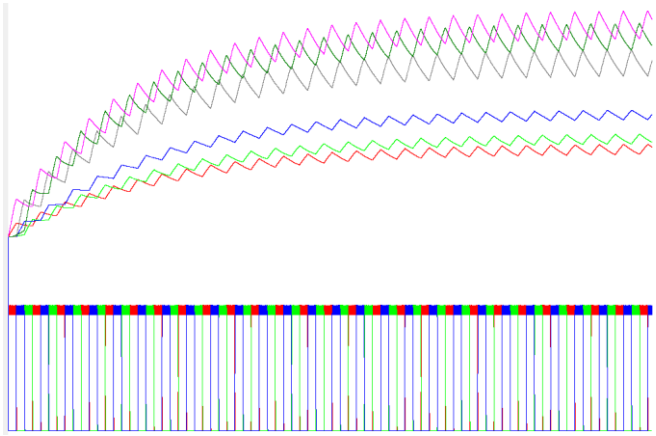

Fig. 9. Operation of the drive in the modified configuration of the power converter.

Running the drive with the proposed active thermal control strategy helps to equalize the temperatures (see Fig. 10) and to decrease the maximum temperature compared to the initial configuration.

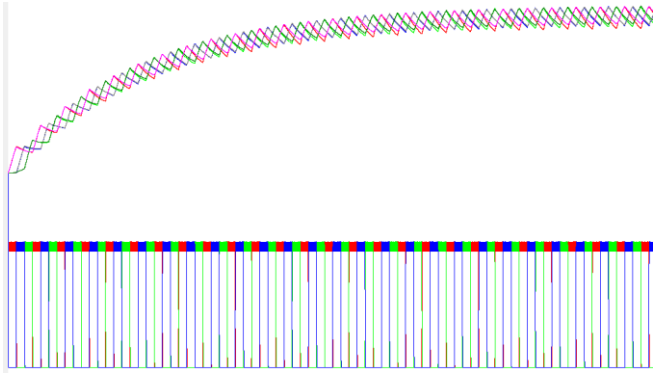

Fig. 10. Operation of the SRD with active thermal control strategy.

V. CONCLUSIONS

The proposed steps of design and algorithmic optimization of the three-phase SRD helps to decrease the maximum temperature of the power modules in the power electronic converter. This allows to increase the output power of the drive before reaching the thermal limits of semiconducting devices.

The proposed solution was verified using a simulation model. Experimental results will be conducted in the future.

REFERENCES

[1] Chetan Urabinahatti ; Syed Shahjahan Ahmad ; G Narayanan, Device loss estimation and heat-sink design for SiC based power converter feeding a switched reluctance machine

[2] V. Blasko, R. Lukaszewski, R. Sladky, “On line thermal model and thermal management strategy of a three phase voltage source inverter,” Conference record of the 1999 IEEE Industry Application Conference. Thirty-Fourth IAS Annual Meeting (Cat. No.99CH36370), Phoenix, AZ, 1999, pp. 1423-1431 vol.2.

[3] D.A. Murdock, J.E.R. Torres, J.J. Connors, R.D. Lorenz, “Active thermal control of power electronic modules,” in IEEE Transactions on Industry Applications, vol. 42, no.2, pp. 552-558, March-April 2006.

[4] M. Andresen, K. Ma, G. Buticchi, J. Falck, F. Blaabjerg and M. Liserre, "Junction Temperature Control for More Reliable Power Electronics," in IEEE Transactions on Power Electronics, vol. 33, no. 1, pp. 765-776, Jan. 2018.

[5] A. Anuchin, V. Ostrirov, Yu. Prudnikova, M. Yakovenko, F. Briz, M. Podlesny, “Thermal stabilization of power devices for compressor drive with start/stop operation mode,” 57th International Scientific

Conference on Power and Electrical Engineering of Riga Technical University (RTUCON), 2016.

[6] T. Kato, K. Inoue, Y. Taniyama, K. Yamada, “Optimum reduction of switching losses based on the two-phase PWM modulation method for two-level inverter”, IEEE 13th Workshop on Control and Modeling for Power Electronics (COMPEL), 2012.

[7] M. C. Di Piazza, M. Pucci, “Efficiency analysis in induction motor drives with discontinuous PWM and electrical loss minimization”, International Conference on Electrical Machines (ICEM), pp. 736-743, 2014.

[8] A. Anuchin, F. Briz, D. Shpak, M. Lashkevich, “PWM strategy for 3-phase 2-level VSI with non-idealities compensation and switching losses minimization,” International Conference on Electric Machines and Drives (IEMDC), 2017.

[9] Alecksey Anuchin ; Dmitry Aliamkin ; Maxim Lashkevich ; Dmitry Shpak ; Alexandr Zharkov ; Fernando Briz, Minimization and redistribution of switching losses using predictive PWM strategy in a voltage source inverter

[10] Shuai Xu ; Hao Chen ; Feng Dong ; Jian Yang, Reliability Analysis on Power Converter of Switched Reluctance Machine System Under Different Control Strategies

[11] Yang Xu ; Hao Chen ; Jason Gu, Power loss analysis for switched reluctance motor converter by using electrothermal model

[12] Alecksey Anuchin ; Daria Grishchuk ; Alexandr Zharkov ; Yulia Prudnikova ; Lidia Gosteva, Real-time model of switched reluctance drive for educational purposes

[13] Fast IGBT4 Modules, SKM100GAL12T4, Semikron, Rev. 1 – 03.09.2013

[14]